X-Ray Attenuation Coefficients from 13 to 80 Mev for Hydrogen, Carbon, Water, and Aluminum

J. M. WYCKOFF AND H. W. KOCH
National Bureau of Standards, Washington, D. C.
(Received September 21, 1959)

The x-ray attenuation coefficients for hydrogen, carbon, water, and aluminum have been measured in the energy range from 13 to 80 Mev by placing varying lengths of attenuators in a 90-Mev bremsstrahlung beam in a good geometry experiment using a large sodium-iodide total-absorption spectrometer as the detector. In the hydrogen case, a difference method employing cyclohexane (C_6H_{12}) and graphite was used. The theoretical attenuation coefficients were calculated using selected Compton and triplet cross sections in addition to the small quasi-deuteron cross sections. A pair cross-section increase of 2.25% was required for carbon, water, and aluminum to bring the total calculated coefficients into agreement with the measured coefficients in the 60-Mev region. The difference between these calculated cross sections and the measured cross sections in the 13- to 50-Mev region has been ascribed to the giant resonance nuclear absorption. A larger high-energy tail to this absorption than predicted by (γ,p) and (γ,n) experiments is indicated.

I. INTRODUCTION

THE paper by Grodstein[1] summarized the theoretical and experimental situation on high-energy and narrow beam attenuation coefficients up to 1957. In that work the theoretical pair production component of the total attenuation coefficient, somewhat inaccurate due to the use of the Born approximation in its calculation,[2] was adjusted to fit experimental data in the 2- to 100-Mev region. While this was successful for high atomic number materials, the fit was poor for low atomic number attenuators with calculated 88-Mev values some 4% lower than Lawson's[3] measurement for copper and aluminum. The recent measurements of Moffatt *et al.*[4,5] which agreed with the Lawson results used the tip of a bremsstrahlung spectrum for total attenuation measurements at 94, 68, and 42 Mev.

In the present experiment,[6] the entire 90-Mev bremsstrahlung spectrum from a synchrotron was measured with a sodium-iodide spectrometer in a good geometry experiment for photon energies from 13 to 80 Mev. The use of this spectrometer combined with the high intensity synchrotron beam made it possible to attenuate the primary x-rays by a factor of over 10 000 with a resulting enhancement of the effect of small changes in the attenuation coefficient. Consequently, the coefficients should be accurate to 1.0% in the region of 25 to 80 Mev with somewhat greater uncertainties in the 13- to 25-Mev region for carbon, water, and aluminum. For hydrogen the difference method employed introduced uncertainties of about 3.3%.

In principle, the broad energy range from 13 to 80 Mev allowed separate evaluation of the electronic and nuclear attenuation processes in those regions where they were important. The particular choice of low-Z attenuators was made in order to emphasize the nuclear absorption as well as make possible an accurate measurement of the electronic attenuation in the 25- to 80-Mev region where it was changing only slowly with energy. The results are shown to be in good quantitative agreement with those of Moffatt *et al.*

II. EXPERIMENTAL ARRANGEMENT AND PROCEDURE

Figure 1 shows the geometry as well as the measuring equipment used. The source of the x-rays was a 180-Mev synchrotron that was operated at 90 Mev for most of the experiments giving good attenuation measurements up to 80 Mev. A few experiments at 35 Mev gave pulse-height distributions that were very sensitive to the nuclear absorption cross sections in the giant resonance region.

As shown in Fig. 1 a primary collimator 0.30 in. in diameter produced a beam 0.70 in. in diameter at the entrance to the attenuator. The attenuator characteristics are listed in Table I. A secondary collimator following the attenuator was 0.59 in. in diameter and was located to restrict the beam striking the 5-in. diameter by 9-in. long sodium-iodide, spectrometer[7] to 0.88 in. in diameter.

After passing through a glass accelerator tube wall of about 4.54 g/cm² the beam was monitored by a multi-

[1] G. White Grodstein, *X-Ray Attenuation Coefficients from 10 kev to 100 Mev*, National Bureau of Standards Circular No. 583 (U. S. Government Printing Office, Washington, D. C., 1957). An earlier unpublished NBS report, 1952, also by G. White Grodstein has been duplicated in the following articles: (a) C. M. Davisson and R. D. Evans, Revs. Modern Phys. **24**, 102 (1952); (b) R. H. Morgan, *Handbook of Radiology* (The Year-Book Publishers, Inc., Chicago, 1955), pp. 99–117; (c) K. Siegbahn, *Beta- and Gamma-Ray Spectroscopy* (Interscience Publishers, Inc., New York, 1955), pp. 857–874. The basic difference between the two Grodstein reports is in the triplet cross sections used. The 1952 report used the Borsellino cross sections, while NBS Circular 583 used the Votruba results. To illustrate the differences, the present experiment at 60 Mev yields a carbon attenuation coefficient of 0.01441 ±1% cm²/g to be compared with 0.0142 cm²/g in the 1952 NBS report and 0.0138 cm²/g in NBS Circular 583.

[2] Davies, Bethe, and Maximon, Phys. Rev. **93**, 788 (1954).

[3] J. L. Lawson, Phys. Rev. **75**, 433 (1949).

[4] Moffatt, Thresher, Weeks, and Wilson, Proc. Roy. Soc. (London) **A244**, 245 (1958).

[5] J. Moffatt and G. C. Weeks, Proc. Phys. Soc. (London) **73**, 114 (1959).

[6] J. M. Wyckoff and H. W. Koch, Bull. Am. Phys. Soc. **3**, 174 (1958).

[7] R. S. Foote and H. W. Koch, Rev. Sci. Instr. **25**, 746 (1954).

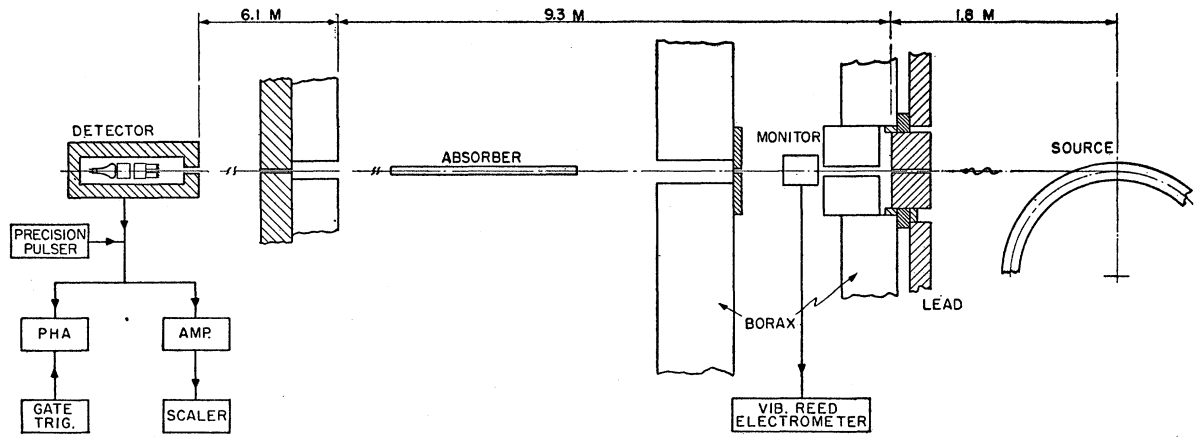

FIG. 1. Experimental geometry and block diagram.

plate, transmission ionization chamber 3.438 g/cm² of aluminum thick. Temperature regulation of the chamber batteries minimized drifts in the vibrating reed electrometer used to measure the collected charge though small corrections were required for experiments with very low x-ray intensities.

The signal from the photomultiplier was fed via a cathode follower to a core memory type, 256 channel, pulse-height analyzer. The stability of this device against drift in channel width and base line was tested daily and proved to be very good. The gain change of the amplifier-analyzer system during any one day's operation was less than $\pm 0.3\%$ while the possible base line drifts of the analyzer were about one channel. The circuit of the analyzer and the 350-microsecond long synchrotron burst prevented pile-up of spectrometer pulses so that the distortion in the experimental pulse-height distributions obtained from the spectrometer was negligible at the spectrometer counting rates of about two counts per synchrotron x-ray burst. A separate fast discriminator and scaler were used with a relatively small and known deadtime to determine the normalization constant of counts per charge collected by the monitor chamber. The spectrometer signal was gated to remove the background of pulses that occurred at times between the synchrotron x-ray bursts.

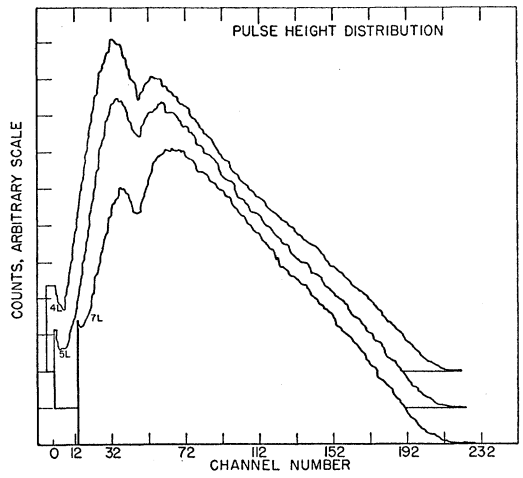

FIG. 2. Raw pulse-height distributions produced by the 90-Mev bremsstrahlung passing through 396.82 ($4L$), 496.43 ($5L$), and 698.86 ($7L$) g/cm² of carbon. These data have been taken directly from the pulse-height analyzer output without corrections for background or channel width.

A series of separate experiments[8] made it possible to calculate and correct for the response functions of the spectrometer. Although the process is described in more detail in the reference cited, it is described briefly here. The response function for a specific photon energy is defined as the frequency distribution of pulses obtained from the spectrometer when bombarded by monoenergetic x-rays. The response functions for all the x-ray energies studied in this experiment were obtained by two procedures. First, in the x-ray energy range from 10 to 20 Mev, information obtained from response functions for monoenergetic electrons permitted a synthesis of the response functions for x-rays. Second, above 20 Mev, the response of the spectrometer to various photon energies was determined by an activation method with bremsstrahlung spectra directed at the spectrometer. The pulse-height distributions produced by the spectra were examined with single fixed channels on the differential analyzer. The contributions of the spectrometer voltage pulses to the single channel depended on the relative energy position of the channel and the maximum energy in the x-ray spectrum. The curve of the number of pulses contributed to a given single channel by various maximum-energy spectra is called the activation curve. The response function was obtained by interpreting the integral expression for the activation curve.

These data on the response function details as obtained by the two methods were used to manufacture

[8] H. W. Koch and J. M. Wyckoff, *Proceedings of the Sixth Scintillation Counter Symposium* [IRE Trans. on Nuclear Sci. NS-5, 127 (1958)].

the 56 element by 56 element matrix describing the response functions that was encoded for use on an electronic computer. Each of the features of the response function such as resolution, area, amplitude and location of the peak with respect to the complete deposition of photon energy in the spectrometer were plotted and smoothed in the construction of the matrix. The basic energy reference for this matrix was the energy deposited in the crystal as obtained experimentally from the 4.43-Mev C^{12} gamma-ray line from a RaD(α,Be) source. The application of this matrix will be discussed in the next section.

III. DATA AND RESULTS

Figure 2 gives the pulse-height distributions as plotted by the pen recorder on the output of the analyzer for three different lengths of carbon. The first step in analyzing these data was to correct for unequal analyzer channel width (a maximum of 9%) and for background. The data were then normalized to a given ionization charge collected on the plates of the monitor chamber. The results are given in Fig. 3. An uncorrected attenuation coefficient may be calculated for each analyzer channel with these data. These coefficients reflect a weighted average of the attenuation coefficients in a broad energy band, since a family of energies, as shown in Fig. 4, contribute to the counts in any given analyzer channel due to the shape of the spectrometer response functions. The correction for this detector response was small at most energies but required a fairly detailed evaluation.

The definition and the determination of the correction factor can be understood from the definition of the attenuation coefficient, τ, in cm^2/g by the equation:

$$\tau=\ln(I_{\text{in}}/I_{\text{out}})/\rho x, \tag{1}$$

where I_{in} is the number of photons incident and I_{out} is the number transmitted by an attenuator, ρ is the density in g/cc, and x is the length of the attenuator in centimeters. The correction factor, A, to obtain this attenuation coefficient from the uncorrected attenuation coefficient, τ_C, is defined by:

$$A=\frac{\tau_I}{\tau_C}=\frac{\tau_I}{\ln(C_{\text{in}}/C_{\text{out}})/\rho x}, \tag{2}$$

where the denominator contains a ratio of counts, $C_{\text{in}}/C_{\text{out}}$, in place of the ratio of photons in Eq. (1). A was calculated from an estimated attenuation coefficient, τ_I, and from the ratio of counts obtained from predicted pulse-height distributions. The predicted distributions for a given attenuator were computed from an assumed bremsstrahlung spectrum, using the τ_I, and the response function matrix. The correction factor for carbon as well as the other attenuators is shown in Fig. 5. It is seen that the correction factors do reflect the assumed nuclear cross sections. Fortunately, the factors

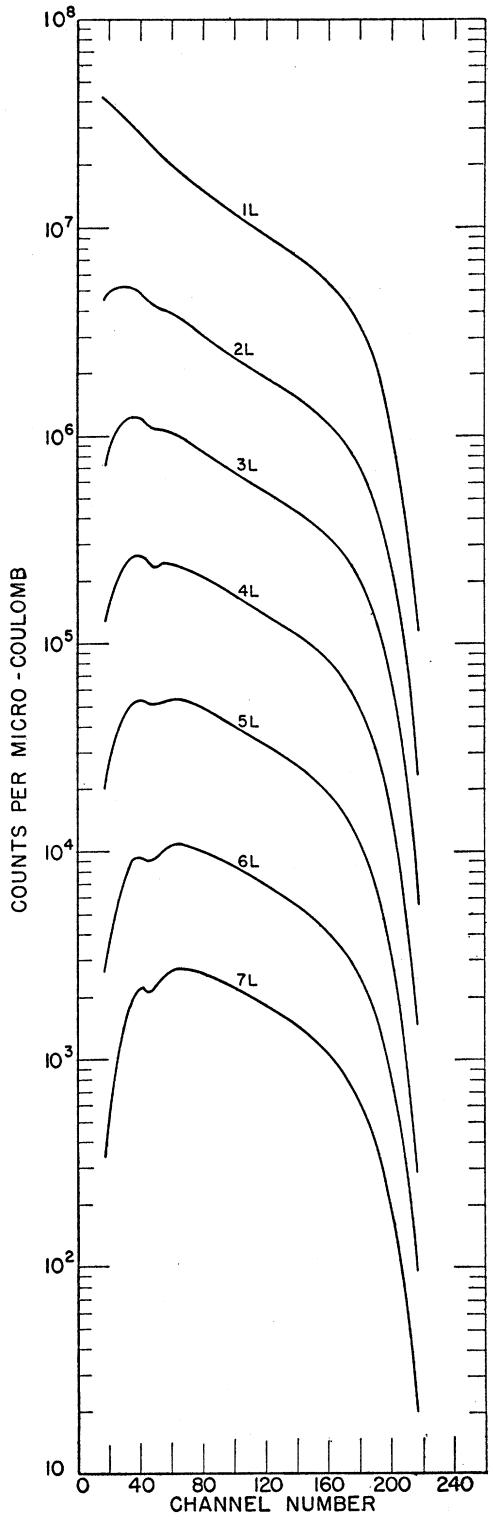

FIG. 3. Pulse-height distributions produced by 90-Mev bremsstrahlung that have passed through seven different lengths of graphite. The absorber characteristics are tabulated in Table I. These curves have been corrected for channel width and background and have been normalized to a common input as measured by the monitor.

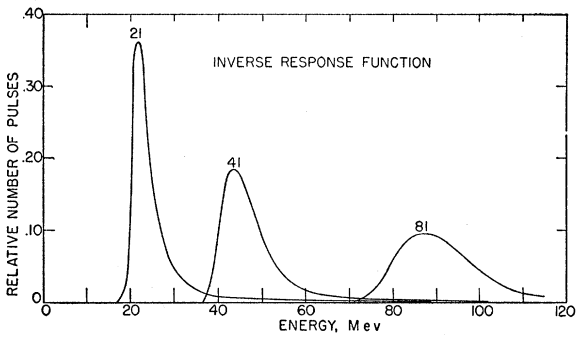

FIG. 4. Three inverse response function curves. These show the photon energies that contribute to the particular pulse heights of 21, 41, and 81 Mev for the 5-in. diameter by 9-in. long NaI(Tl) spectrometer. The data for each curve is taken from one row of the response function matrix.[8] The columns of this matrix are the response functions.

are small ratios even at the giant resonance energies, and, therefore, are relatively insensitive to the assumptions on spectra, attenuation coefficients, and response-function shapes. The application of the factors for carbon to the uncorrected attenuation coefficients obtained from Fig. 3 results in the fully corrected attenuation coefficients for carbon shown in Fig. 6.

As a test of the sensitivity of this procedure to the assumed attenuation coefficients the fully corrected coefficients if Fig. 6 were used to recalculate the response function correction factors. As new factors were only slightly different than those used in Fig. 3 and were within the uncertainties listed in Table III only the original values were used in this paper.

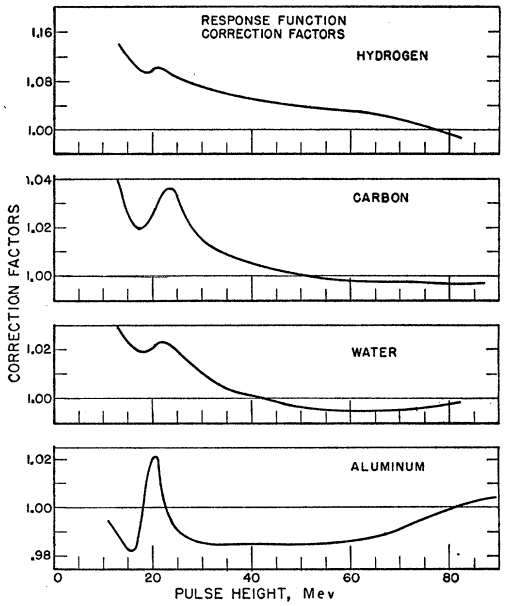

FIG. 5. Response function correction factors for the attenuation coefficients obtained from the pulse-height distributions for hydrogen, carbon, water, and aluminum. These factors have been calculated using assumed coefficients and the response function matrix to predict the pulse-height distributions.

As shown in Table I, the experimental effort emphasized carbon for which seven different lengths were used. A least-squares fit to the logarithm of the resulting experimental counts versus carbon length gave uncorrected ratios of counts per channel that were well determined. The experiments with other attenuators were referred to the pulse-height distributions obtained with one specific length of carbon in order to improve the accuracy. The data obtained with the reference length of carbon were used to extrapolate the pulse-height distributions to the zero attenuator situation by means of the detailed carbon experiments. This procedure made it unnecessary to

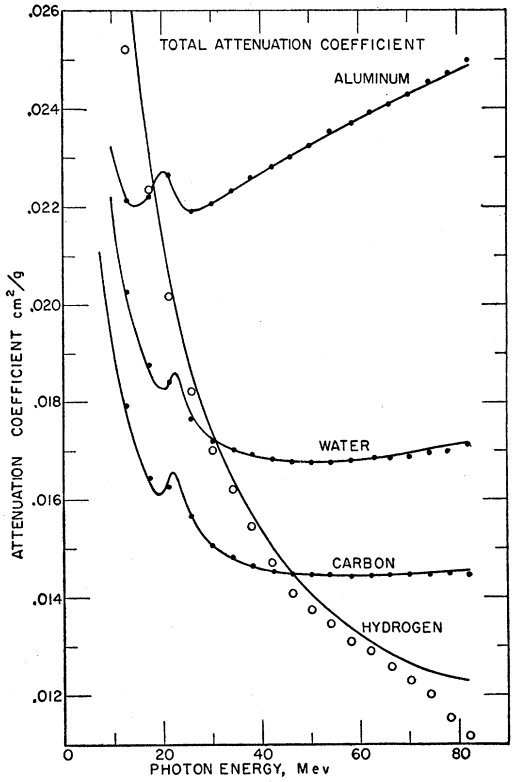

FIG. 6. Predicted attenuation coefficients (solid lines) (see text) and experimental points for hydrogen, carbon, water, and aluminum.

measure the pulse-height distribution for an unfiltered x-ray beam in terms of an absolute monitor current. The drift corrections to this monitor current would have been large due to the small photon flux required to prevent jamming the spectrometer. The drifts would have made the measurements difficult. Consideration of this method will show that the attenuation coefficients of water and aluminum are only slightly sensitive to the uncertainties in density, lengths, or assumed attenuation coefficients of the carbon attenuators.

The procedure for hydrogen was slightly different than that for the other materials. The hydrogen attenuation coefficient was obtained from a ratio of the

photons transmitted by graphite and cyclohexane (C_6H_{12}) attenuators containing the same number of carbon atoms. The difference in the attenuators was 82.7 g/cm² for hydrogen. Although this thickness was equivalent to 11.8 meters of liquid hydrogen, it was much less in g/cm² than the thickness of the other attenuators used. The probable accuracy of the hydrogen results is less than that for the other attenuators because of the small thickness of hydrogen, the poorer statistical accuracy in a subtraction method involving two large quantities, and the relatively rapid change in the attenuation coefficient with energy.

The fully corrected experimental coefficients for hydrogen, carbon, water, and aluminum are tabulated in Table II and shown in Fig. 7(a), (b), (c), and (d). A predicted coefficient that will be discussed in the next section is also drawn on these figures.

TABLE I. Summary of attenuation coefficient experiments.[a]

Symbol	Length g/cm²	Dimensions inches	Synchrotron energy Mev	Time minutes
		Carbon		
0	0		90	30
1*L* carbon	107.13	2.0 diam	90	128
2*L* carbon	215.92	2.0	90	133
3*L* carbon	306.15	2.0	90	149
4*L* carbon	396.82	2.0	90	136
5*L* carbon	496.43	2.0	90	114
6*L* carbon	604.81	2.0	90	160
7*L* carbon	698.86	2.0	90	142
BG carbon +4-in. Pb	698.86	2.0	90	14
	0		34.2	129
Carbon	351.5	2.0	34.2	654
		Aluminum		
Aluminum	427.71	1.5×1.625	90	187
Carbon	527.42	2.0 diam	90	207
		Water		
Water	461.50	2.0625 i.d.	90	184
Carbon	527.42	2.0 diam	90	207
		Hydrogen		
Cyclohexane	579.07	2.0625 i.d.	90	236
Carbon	496.43	2.0 diam	90	114

[a] Liquids were in aluminum tubes; carbon was in the form of graphite rods; aluminum was in the form of extruded bars.

An additional method of determining the coefficient was the detailed prediction of the shapes of pulse-height distributions produced by x rays transmitted by one particular length of absorber. The predictions allowed a sensitive test of the magnitude and a test of the shape, within limitations imposed by the resolutions of the spectrometer, of the giant resonance nuclear cross sections around 20 Mev. For these tests, the synchrotron was operated at about 35 Mev to produce pulse-height distributions of very excellent counting statistics. The results without an attenuator are shown in Fig. 8 and are compared with a predicted curve. Experiments were performed with this same 35-Mev bremsstrahlung spectrum with an absorber of 351.5 g/cm² of carbon and the results are plotted in Fig. 9. The comparisons in Figs. 8 and 9 with the predicted spectra are good and justify the assumptions to be discussed in Sec. VI-D.

TABLE II. Experimental attenuation coefficients in cm²/g.

Energy, Mev	Carbon	Aluminum	Water	Hydrogen
13.3	0.01795	0.02213	0.02026	0.02521
17.5	0.01648	0.02219	0.01883	0.02239
21.5	0.01626	0.02268	0.01846	0.02018
25.9	0.01566	0.02193	0.01766	0.01822
30.3	0.01507	0.02208	0.01721	0.01702
34.3	0.01482	0.02231	0.01701	0.01622
38.3	0.01465	0.02259	0.01693	0.01546
42.3	0.01453	0.02279	0.01684	0.01472
46.3	0.01446	0.02300	0.01677	0.01409
50.3	0.01440	0.02322	0.01675	0.01375
54.3	0.01440	0.02351	0.01676	0.01347
58.3	0.01440	0.02367	0.01681	0.01310
62.3	0.01442	0.02392	0.01685	0.01293
66.2	0.01442	0.02409	0.01685	0.01258
70.2	0.01442	0.02429	0.01687	0.01233
74.2	0.01445	0.02454	0.01696	0.01203
78.2	0.01445	0.02472	0.01699	0.01155
82.2	0.01447	0.02500	0.01711	0.01116

IV. ESTIMATE OF ERRORS IN THE EXPERIMENTAL ATTENUATION COEFFICIENTS

Examples of the magnitudes of the major sources of error are given in Table III for hydrogen, carbon, water, and aluminum and for the photon energy regions, below and above 30 Mev. The statistical errors in standard deviations have been multiplied by 3 to convert them to maximum errors in order to combine the errors by quadrature with the systematic errors. The systematic errors are inherently maximum error estimates.

As can be seen from the table, the density correction has introduced a large uncertainty. The nonuniformities in the graphite attenuator rods were investigated for us by C. T. Collett of the NBS Density group who had one sample rod cut into six lengths. Three of these lengths were turned down from 2-in. diameter to 1.25-in. and then to 0.75-in. diameter. The longitudinal variations in density of less than 0.6% did not affect the measured

TABLE III. Sources of error and estimates of uncertainties.

Material	Energy range Mev	Statistics %	Response function, % Density %	Energy uncertainty	Correction factor	Total %
Hydrogen	13–30	2.4	1.4	0.9	1.6	3.3
	30–80	2.4	1.4	1.6	0.3	3.2
Carbon	13–25	0.8	0.2	0.0	0.7	1.1
	25–30	0.8	0.2	0.4	0.4	1.0
	30–80	0.8	0.2	0.3	0.2	0.9
Water	13–25	0.9	0.1	0.0	0.6	1.1
	25–30	0.9	0.1	0.3	0.3	1.0
	30–80	0.9	0.1	0.3	0.2	1.0
Aluminum	13–25	0.9	0.1	0.0	0.4	1.0
	25–30	0.9	0.1	0.1	0.3	1.0
	30–80	0.9	0.1	0.5	0.3	1.1

attenuation. However, the central zone through which the x-rays passed had a mean density of 1.6637 compared to 1.6640 for the 1.25-in. sample and 1.6809 for the full 2-in. sample. Thus a 1.0% correction was applied to the gross density measurements of the graphite rods with an uncertainty of ±0.2% estimated to account for nonuniformity from rod to rod. The density determination for the aluminum attenuator had an assigned uncertainty of ±0.002%. Due to the "difference method" used for the measurements of the hydrogen

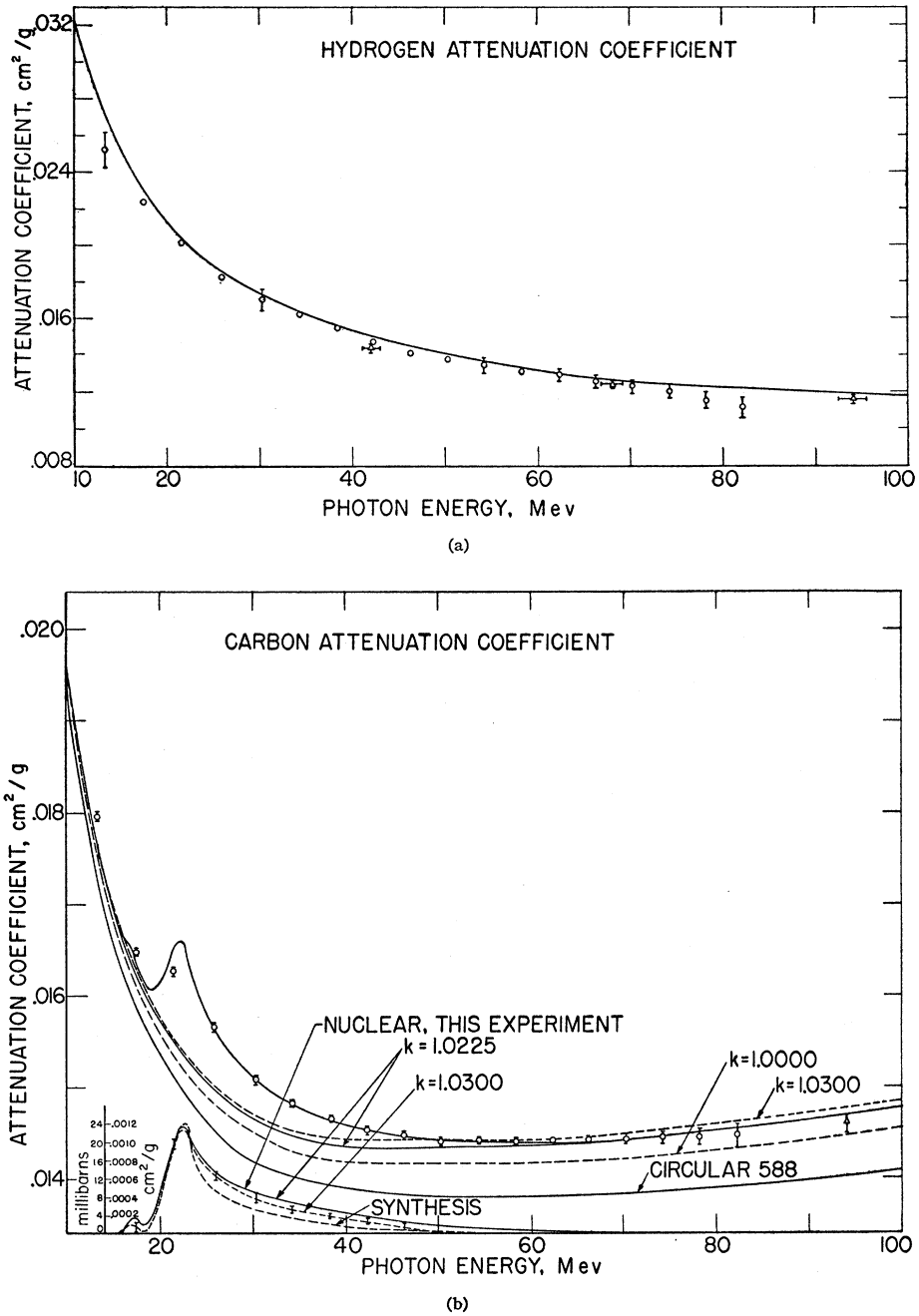

FIG. 7. Detailed plot of attenuation coefficients for (a) hydrogen, (b) carbon, (c) water, and (d) aluminum showing the predicted curves electronic (see text) and the experimental curves. The maximum error is indicated on (a) while only the statistical accuracy is indicated on (b), (c), and (d). The results of the Circular 583 carbon calculation are shown. The carbon curve has been plotted for a pair correction factor of 1.000 and 1.0300 in addition to the value 1.0225 used for the water and aluminum curves. The synthesis of a nuclear cross section is shown for carbon, water, and aluminum as well as the experimental nuclear cross section. The latter was obtained by subtracting the predicted curve for the electronic processes only from the experimental points. Experimental points of Lawson[3] at 88 Mev and Moffatt *et al.*[4,5] at 94, 68, and 42 Mev are shown by triangles as are some of the lower energy results tabulated in reference 1.

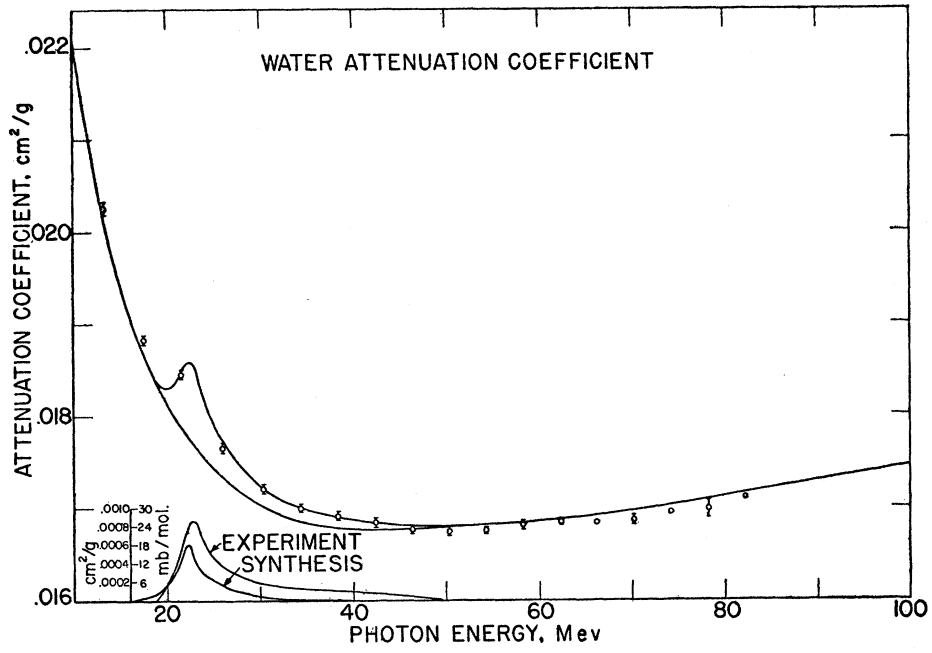

(c)

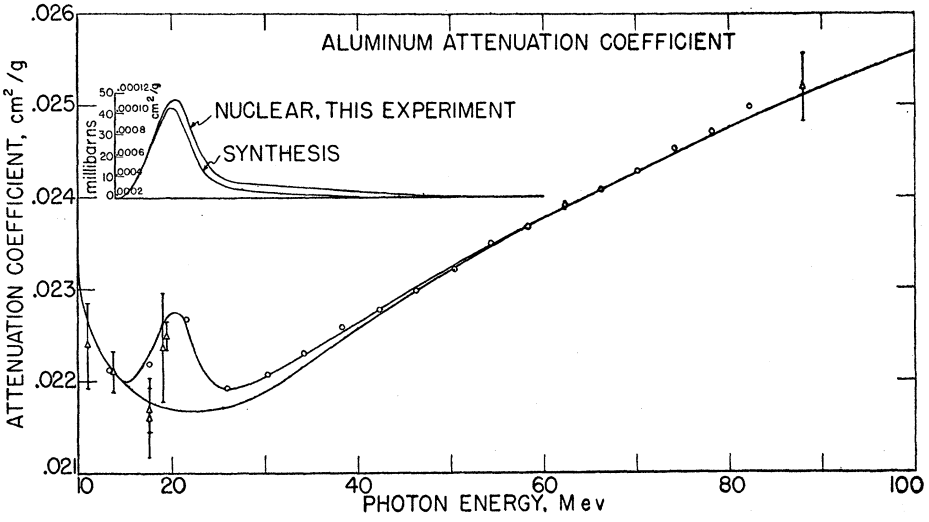

(d)

FIG. 7.—*Continued*

coefficient, the uncertainty due to the carbon density had a large effect on this particular coefficient.

The estimates of the uncertainties in the attenuation coefficient due to uncertainties in the response-function correction factor have been subdivided into two contributions in Table III. The first estimate listed as "Response function (Energy uncertainty)" results from an assumption of a $\pm 2\%$ energy uncertainty in the synchrotron energy calibration which influences the assignment of energies in the response function matrix above 30 Mev as previously described in the discussion of the two methods for obtaining the response functions. In the energy range from 25 to 30 Mev, this uncertainty in the attenuation coefficients due to this energy uncertainty was assumed to be half as large as that above 30 Mev. Below 25 Mev no uncertainty was assumed. The second uncertainty labelled "Response function (Correction factor)" was due to the uncertainty in the response-function correction factor which was taken to be $\frac{1}{5}$ of the percentage correction factor.

While the uncertainties listed below 25 Mev are not appreciably larger than those above this energy, it should be noted that the sensitivity of the response function correction factor to the assumed giant reso-

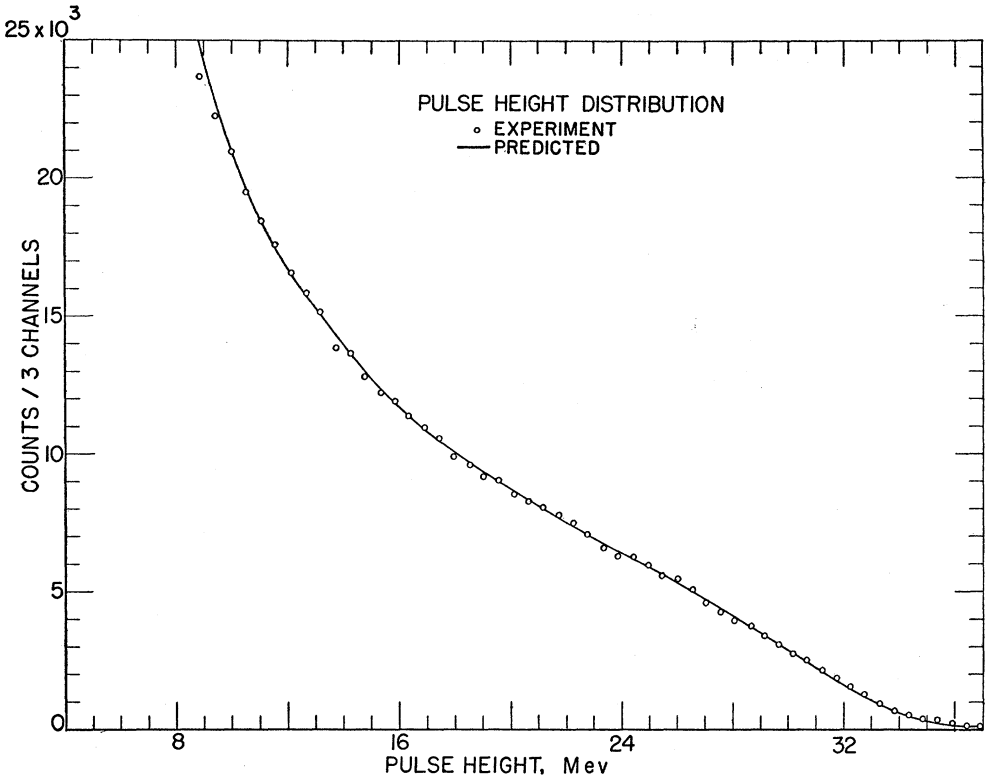

FIG. 8. The predicted pulse height distribution (solid line) for a 35.3-Mev bremsstrahlung spectrum passing through the donut wall and monitor ionization chamber to strike a 5-in. diameter by 9-in. long NaI(Tl) total absorption spectrometer. A Davies-Bethe-Maximon[2] spectrum using Hisdal's[35] target correction was assumed in the prediction. The plotted experimental points have been corrected for channel width, and background was negligible. The predicted curve has an arbitrary vertical normalization.

nance is largest in this region and that in addition the broad response function of the crystal makes it impossible to resolve fine detail in this region. These sources of uncertainty have not been appraised in detail here but should be borne in mind in the interpretation of the giant resonance region.

The small sources of error of recombination of the ions in the monitor chamber and photon inscattering effects for the present geometry were less than 0.05%. Uncertainties introduced by electrometer drift, channel width changes, electrometer condenser measurement, liquid temperature corrections and attenuator material impurities were negligible.

V. PREDICTIONS OF THE TOTAL ATTENUATION COEFFICIENTS

The predictions of Tables IV(a) and (b) that are shown in Figs. 7(a), (b), (c), and (d) will be described in detail in this section. The major attenuation processes from 30 to 80 Mev for which there are theoretical predictions—pair production, triplet production, Compton scattering, and nuclear absorption by the quasi-deuteron process—are discussed in part *A*. The nuclear processes that are important in the giant resonance region around 20 Mev will be discussed in part *B*.

A. Electronic and Quasi-Deuteron Contributions

1. Pair Production

The major contribution to the total cross section for carbon, water, and aluminum is pair production in the field of the nucleus. Calculations of this cross section for nonscreened nuclei were made by using Bethe-Ashkin's[9] formula 110, originally derived by Bethe-Heitler.[10] This formula gives cross sections for carbon in millibarns that are 76.28 (10 Mev), 110.08 (15 Mev), 117.14 (20 Mev), 141.48 (30 Mev), 161.13 (40 Mev), 174.96 (50 Mev), 186.23 (60 Mev), 204.41 (80 Mev), and 218.74 (100 Mev). Other materials go as the ratio of their Z^2 values. These values should be more accurate and at 60 Mev are about 1% below those that are evaluated by using the nonscreened version of the simpler expression, Bethe-Ashkin's[9] formula 114.

The pair cross section listed for hydrogen was calculated using formula 114. A comparison of the 60-Mev result with a more accurate formula 110 calculation with a screening correction showed the results listed here to be about 1% low. As the pair contribution to the hydrogen cross section was small this was considered acceptable. No correction was made for effects on the hydrogen coefficient of the cyclohexane molecular binding since the correction is negligible. These effects will reduce the screening correction which is only 1% at 60 Mev.

Two corrections to the nonscreened cross sections for

[9] H. A. Bethe and J. Ashkin, in *Experimental Nuclear Physics*, edited by E. Segrè, Vol. I (John Wiley and Sons, Inc., New York, 1953), 1st ed., pp. 326, 327. These formulas were evaluated with the help of R. A. Schrack to whom we are indebted.

[10] H. A. Bethe and W. Heitler, Proc. Roy. Soc. (London) **A146**, 83 (1934).

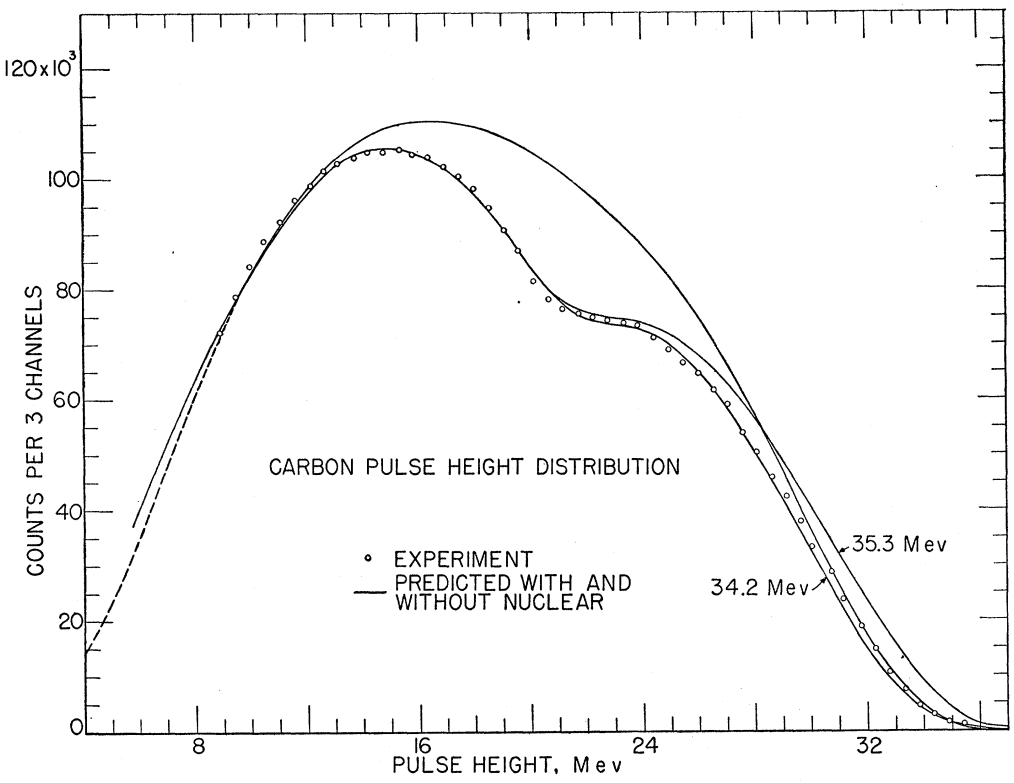

FIG. 9. The pulse-height distribution (solid line) predicted for 34.2- and 35.3-Mev bremsstrahlung that have passed through 351.5 g/cm² of carbon to enter a 5-in. diameter by 9-in. long NaI(Tl) total absorption spectrometer. The electronic attenuation processes only yield the top curve; the inclusion of the "experimental" nuclear cross section yields the lower curves. Plotted experimental points have been corrected for channel width and background (dotted line). The vertical normalizations of the predicted curves are arbitrary.

other attenuators must be considered. The Coulomb correction of Davies, Bethe, and Maximon[2] has been applied and is everywhere below 0.4%. The screening correction was based on the form factor obtained from the Hartree self-consistent field model.[11,12] This correction makes the pair cross section at 60 Mev for carbon larger by 0.5% than that obtained from a Thomas-Fermi screening correction.

As is noted in Table IV(a), the corrected pair cross sections for carbon, oxygen, and aluminum were multiplied by a constant $K=1.0225$. This constant was justified by comparing the experimental counts per charge for lengths of carbon and aluminum containing equal numbers of electrons. The ratio of the transmitted x-ray intensities should depend only on the difference of the pair cross sections of these materials, since the Z-dependent cross sections for the Compton, triplet, and quasi-deuteron processes and their corrections should drop out. A correction for the detector response function was required to convert the ratio of the counts to the ratio of the photons measured. It was found that at 60 Mev an increase of more than 2% to both the carbon and aluminum theoretical pair cross sections was required in order to predict the experimental ratio of photons. This experiment suggested that the pair cross section is the major one to be modified in order to provide a consistent agreement with the experimental total attenuation coefficients.

The pair production cross section has been assumed to be in error for lack of a better hypothesis. However any nuclear or electronic process that depends on a power of Z greater than one would produce the same effect found in this experiment.

2. *Triplet Production*

Widely varying results have been obtained by several authors who have calculated the cross section for the production of pairs in the field of electrons (triplets). Votruba[13] and Joseph and Rohrlich[14] have predicted the lower cross sections shown on Fig. 10. Recent calculations by Suh and Bethe[15] at Cornell and experimental work of Malamud,[16] and Hart *et al.*[17] at that laboratory have shown a closer agreement with the early calculation of Wheeler and Lamb[18] of a higher cross section particularly at energies above 100 Mev.

[11] A. T. Nelms and I. Oppenheim, J. Research Natl. Bur. Standards **55**, 53 (1955).

[12] We are indebted to R. T. McGinnies for performing this calculation at 60 Mev for carbon and aluminum. The correction was subsequently applied to the Thomas-Fermi correction at all energies.

[13] V. Votruba, Phys. Rev. **73**, 1468 (1948); Bull. intern. acad. tchéque sci., Prague **49**, 19 (1948).

[14] J. Joseph and F. Rohrlich, Revs. Modern Phys. **30**, 354 (1958).

[15] Kiu S. Suh and H. A. Bethe, Bull. Am. Phys. Soc. Ser. II, **4**, 13 (1959) and Phys. Rev. **115**, 672 (1959).

[16] E. Malamud, Phys. Rev. **115**, 687 (1959).

[17] Hart, Cocconi, Cocconi, and Sellen, Phys. Rev. **115**, 678 (1959).

[18] J. A. Wheeler and W. E. Lamb, Jr., Phys. Rev. **55**, 858 (1939).

TABLE IV. Calculated attenuation coefficients.

Energy Mev	Compton[a] barns	Pair[b] barns	Triplet[c] barns	Nuclear[d] giant res. barns	Quasi-deuteron[e] barns	Total with nuclear barns	Total with nuclear cm²/g	Total without nuclear barns	Total without nuclear cm²/g
			Hydrogen				$R=0.5997$[f]		
10	0.0510	0.0021	0.0011			0.0542	0.03250		
15	0.0377	0.0027	0.0018			0.0422	0.02531		
20	0.0302	0.0032	0.0023			0.0357	0.02141		
30	0.0220	0.0039	0.0031			0.0290	0.01739		
40	0.01746	0.0044	0.0037			0.0256	0.01535		
50	0.01456	0.0048	0.0041			0.0235	0.01409		
60	0.01254	0.0051	0.0045			0.0221	0.01325		
80	0.00988	0.0056	0.0051			0.0206	0.01235		
100	0.00820	0.0060	0.0056			0.0198	0.01187		
			Carbon				$R=0.05016$		
10	0.3060	0.0775	0.0070			0.3905	0.01959		
15	0.2260	0.1013	0.0110	0.0		0.3383	0.01697	same	
20	0.1814	0.1181	0.0140	0.0080		0.3215	0.01613	0.3135	0.01573
30	0.1319	0.1415	0.0190	0.0090	0.0000	0.3014	0.01512	0.2924	0.01467
40	0.1048	0.1590	0.0220	0.0048	0.0004	0.2910	0.01460	0.2862	0.01436
50	0.0874	0.1727	0.0250	0.0016	0.0012	0.2879	0.01444	0.2863	0.01436
60	0.0752	0.1828	0.0270	0.0010	0.0015	0.2875	0.01442	0.2865	0.01437
80	0.0593	0.1987	0.0300	0.0	0.0016	0.2896	0.01453	same	
100	0.0492	0.2107	0.0333		0.0014	0.2946	0.01478		
			Oxygen				$R=0.03765$		
10	0.4080	0.1369	0.0093			0.5542	0.02087		
15	0.3020	0.1791	0.0150	0.0		0.4961	0.01868	same	
20	0.2420	0.2097	0.0190	0.0045		0.4752	0.01789	0.4707	0.01772
30	0.1759	0.2507	0.0250	0.0057	0.0000	0.4573	0.01722	0.4516	0.01700
40	0.1397	0.2813	0.0290	0.0030	0.0005	0.4535	0.01707	0.4505	0.01696
50	0.1165	0.3051	0.0330	0.0010	0.0015	0.4561	0.01718	0.4561	0.01717
60	0.1003	0.3219	0.0360	0.0	0.0020	0.4602	0.01733	same	
80	0.0790	0.3501	0.0400		0.0021	0.4712	0.01774		
100	0.0656	0.3711	0.0440		0.0018	0.4825	0.01817		
			Aluminum				$R=0.02233$		
10	0.6630	0.3611	0.0150	0.0		1.0391	0.02320	same	
15	0.4900	0.4707	0.0230	0.0013		0.9850	0.02200	0.9837	0.02197
20	0.3930	0.5489	0.0300	0.0466		1.0185	0.02274	0.9719	0.02170
30	0.2860	0.6542	0.0400	0.0072	0.0000	0.9874	0.02205	0.9802	0.02189
40	0.2270	0.7339	0.0480	0.0049	0.0003	1.0133	0.02263	1.0092	0.02254
50	0.1893	0.7962	0.0530	0.0009	0.0019	1.0413	0.02325	1.0404	0.02323
60	0.1630	0.8409	0.0580	0.0	0.0032	1.0651	0.02378	same	
80	0.1284	0.9106	0.0660		0.0036	1.1086	0.02476		
100	0.1065	0.9639	0.0720		0.0031	1.1455	0.02558		
			Water				$R=0.03344$		
10						0.6626	0.02216	0.6626	0.02216
15						0.5805	0.01941	0.5805	0.01941
20						0.5466	0.01828	0.5421	0.01813
30						0.5153	0.01723	0.5096	0.01704
40						0.5047	0.01688	0.5017	0.01678
50						0.5031	0.01682	0.5031	0.01682
60						0.5043	0.01686	0.5043	0.01686
80						0.5124	0.01713	0.5124	0.01713
100						0.5221	0.01746	0.5221	0.01746

[a] Compton-Klein-Nishina.
[b] Pair (Unscreened Bethe and Heitler—Hartree screening—Coulomb corrections). This was multiplied by 1.0225 for C, O, and Al.
[c] Triplet—Borsellino.
[d] Nuclear—experimental (see text).
[e] Quasi-deuteron—Levinger with Danos quenching from Whalin exp.
[f] Conversion factor—$R=(\text{cm}^2/\text{g})/(\text{barns/atom})$.

In the present synthesis the calculation of Borsellino,[19] which is intermediate between these two extremes, has been used as the basis of the triplet calculation. His calculation approaches Wheeler and Lamb in the high-energy region and Votruba in the lower energy region of this experiment.

3. *Compton Scattering*

The cross section included for this process was calculated by the Klein-Nishina formula for free electrons as tabulated in NBS Circular 583.[1]

[19] A. Borsellino, Helv. Phys. Acta **20**, 136 (1947); Nuovo cimento **4**, 112 (1947).

4. *Photoelectric and Other Electronic Attenuation Processes*

No electronic processes other than those discussed above were included in the theoretical prediction. Most of the additional effects are either small or could not be included properly. For example, (a) the photoelectric cross section is 2.4×10^{-31} cm^2 per atom for carbon at 15 Mev which is negligibly small; and (b) the Delbruck scattering cross section is about 10^{-31} cm^2 per atom for aluminum at 60 Mev. Other effects, such as (c) atomic binding effects in the Compton process, and (d) Rayleigh scattering by the atomic electrons are also expected to be small.

The main effects that have not been included adequately are (e) the radiative corrections to the pair and Compton processes including the double Compton process.[20,21] These corrections to the differential cross sections in experiments with good energy resolution (of the order of 100 kev) and good geometry will be large. For example, Brown and Feynman[21] estimate the Compton cross section correction at zero degrees (where the double Compton cross section is zero) will decrease the cross section by 3.8% at a photon energy of 50 Mev and 5.3% at 150 Mev. Also, Bjorken, Drell, and Frautschi[22] show that the large-angle pair cross section will have a radiative correction less than 5%. However, in the present experiment, the corrections of interest are those that change the integrated cross section for *removal* of photons from the detector. The present detector arrangement has the characteristics of good geometry but relatively poor energy resolution. For this case, the radiative corrections to the total attenuation cross sections are uncertain as to sign and magnitude as far as the present authors have been able to determine.

In spite of the possible importance of the radiative corrections, the predicted attenuation coefficients were calculated without the radiative corrections and without the other electronic processes (a) to (d).

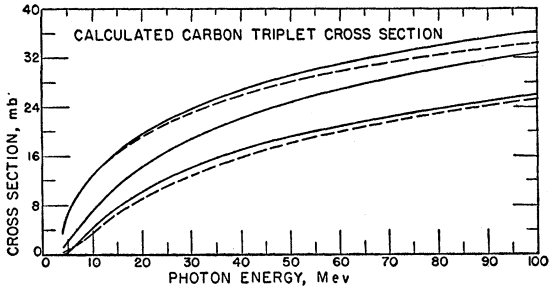

FIG. 10. Five different carbon triplet cross section predictions. From top to bottom they are (a) Wheeler and Lamb,[18] (b) $(1/Z)$ times the corrected pair cross section, (c) Borsellino,[19] (d) Wheeler and Lamb with an exchange correction suggested by Joseph and Rohrlich,[14] and (e) Votruba.[13]

[20] W. Heitler, *The Quantum Theory of Radiation*, (Clarendon Press, London, 1954), 3rd ed., p. 227.
[21] L. M. Brown and R. P. Feynman, Phys. Rev. **85**, 231 (1952).
[22] Bjorken, Drell, and Frautschi, Phys. Rev. **112**, 1409 (1958).

TABLE V. Photonuclear cross-section data.

Isotope	Reaction	Energy range	Cross section	Reference
C^{12}	(γ,n)	19–38 Mev	Absolute	30
	(γ,p)g.s.	16.5–24 Mev	Absolute	28
	(γ,p)g.s.	24–50 Mev	Absolute	29
O^{16}	(γ,n)	16–22.5 Mev	Absolute plus extrapolation to 23 Mev	31
	(γ,p)	18–25 Mev	Absolute	28
	(γ,p)g.s.	23–45 Mev	Shape normalized to total absolute σ at 23 Mev	29
Al^{27}	(γ,n)	16–22 Mev	Absolute	32
	(γ,p)	15–24 Mev	Absolute	33
	(γ,p)g.s.	22.5–40 Mev	Shape normalized to total absolute σ at 22.5	29

5. *Quasi-Deuteron Production*

Levinger[23] has proposed that the quasi-deuteron cross section may be calculated by the formula $\sigma_{qd} = (6.4NZ\sigma_d)/A$ for high energies. Barton and Smith[24] found that this expression was in agreement with their measurements on helium and lithium with 280-Mev bremsstrahlung. Danos[25] has calculated an approximate quenching factor that reduces this cross section to 40% of this value for carbon at 50 Mev and 30% for aluminum at this energy. Based on the deuteron cross-section measurements of Whalin *et al.*,[26] the quasi-deuteron cross section listed in Table IV were calculated using this quenching factor. The relatively small values of this component as well as the variation with Z similar to the triplet cross section makes it difficult to evaluate the correctness of this calculation from this experiment.

B. Nuclear Attenuation Processes in the Giant Resonance Region

The only important nuclear processes[27] in the energy range from 13 to 40 Mev are those leading to neutron and proton production. Unfortunately, the only complete data on these processes are for carbon. Table V gives the references[28–33] for this and other materials for

[23] J. S. Levinger, Phys. Rev. **84**, 43 (1951).
[24] M. Q. Barton and J. H. Smith, Phys. Rev. **110**, 1143 (1958).
[25] M. Danos, Bull. Am. Phys. Soc. Ser. II, 4, 102 (1959); and private communication.
[26] Whalin, Schriever, and Hanson, Phys. Rev. **101**, 377 (1956).
[27] The photoalpha production process is reported by F. K. Goward and J. J. Wilkins, *Cross Sections for the Photo-Disintegrations* $^{12}C(\gamma,3\alpha)$ *and* $^{16}O(\gamma,4\alpha)$, Atomic Energy Research Establishment Memorandum *G/M*127 (Ministry of Supply, Harwell, 1952); It has a maximum of 0.4 millibarn and was not included in these calculations. Similarly the (γ,γ) process with a 0.1 millibarn maximum was neglected.
[28] Cohen, Mann, Patton, Reibel, Stephens, and Winhold, Phys. Rev. **104**, 108 (1956).
[29] S. Penner and J. E. Leiss, Phys. Rev. **114**, 1101 (1959); Bull. Am. Phys. Soc. **3**, 56 (1958); and private communication.
[30] Barber, George, and Reagan, Phys. Rev. **98**, 73 (1955).
[31] Katz, Haslam, Horsley, Cameron, and Montalbetti, Phys. Rev. **95**, 464 (1954).

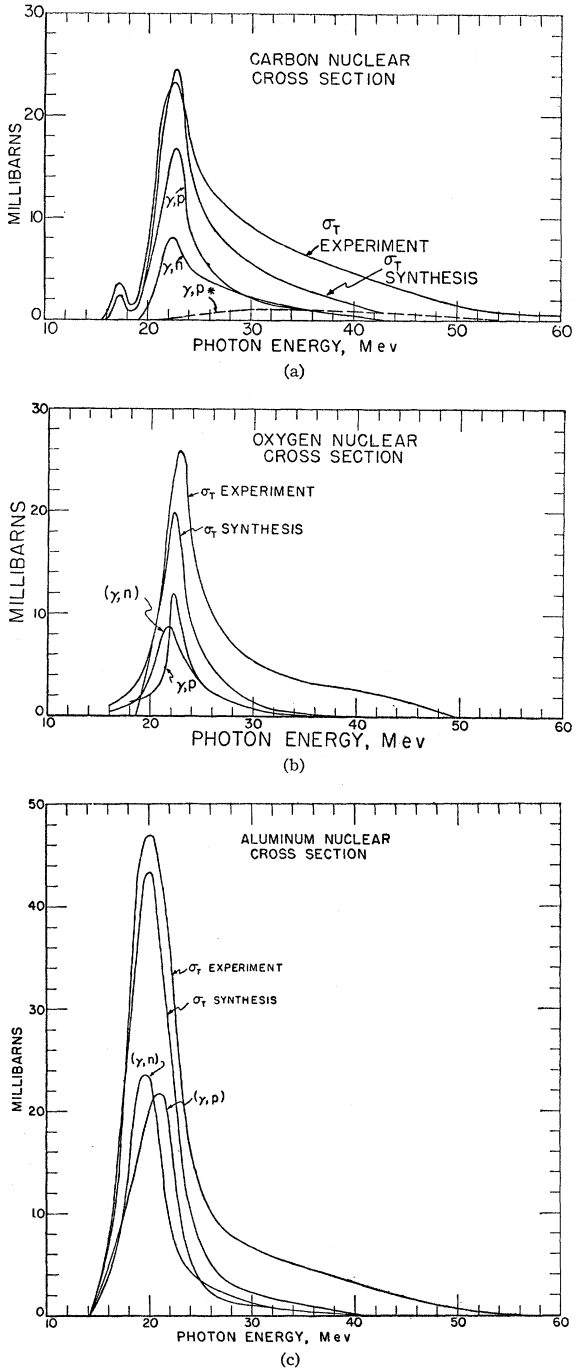

FIG. 11. The (γ,n), (γ,p), and (γ,p^*) components of the total nuclear cross sections. The sum of these is labeled "synthesis" and the experimental cross sections (see text) are shown for (a) carbon, (b) oxygen (water), and (c) aluminum. The references for these data are listed in Table V.

which the nuclear cross section has been synthesized. For carbon-12 the photoproton cross sections used up to 24 Mev which presumably correspond only to ground-state transitions in the boron-11, are those given by Cohen *et al.*[28] At energies above 21 Mev it is necessary to include the excited state transitions as measured by Penner and Leiss.[29] The photoneutron cross sections measured by Barber, George, and Reagan[30] by a study of the 20-minute carbon-11 radioactivity automatically include both the ground- and excited-state transitions. However, the $(\gamma,2n)$ cross section with a threshold of 32 Mev would not be included.

The oxygen (γ,p) and (γ,n) data of Cohen *et al.*[28] and Katz *et al.*,[31] respectively, were used in the synthesis of a total nuclear cross section up to 23 Mev. Above 23 Mev the shape of the (γ,p) cross section corresponding to ground-state transitions found by Penner and Leiss was used to provide the total nuclear cross section by normalizing their cross section to the lower energy data at 23 Mev. The same procedure was followed for aluminum by using the relative cross sections found by Penner and Leiss for ground-state transitions with a normalization at 22.5 Mev. The resulting predictions are marked "synthesis" in Fig. 7 and Fig. 11.

The experimental, "nuclear absorption" curves shown on these figures result from a subtraction of the predicted electronic and quasi-deuteron components from the experimental total attenuation coefficient. Above the energies of the giant resonance peak, the experimental total attenuation coefficient given by the points on the figures were obtained as described in Sec. III. At the giant resonance energies these same data are available and are shown on the figures. However, greater reliance in the giant-resonance energy region was placed on the shape and magnitude of the total coefficient obtained from detailed matching of pulse-height distributions as demonstrated in Fig. 9. Therefore, the experimental data in the solid curves drawn at the top of Fig. 7(a)–(d) do not necessarily pass through all the experimental points obtained from the attenuation experiments with different attenuator lengths. In those cases, the solid curve is regarded as the experimental result.

VI. DISCUSSION OF RESULTS

A. Total Cross Sections in the Energy Range from 30 to 80 Mev

The most accurate results from this experiment are the total cross sections in the energy range from 30 to 80 Mev where the cross section varies slowly with energy and the spectrometer resolution corrections are small. When a comparison of the experimental points in Fig. 7(a), (b), (c), and (d) are made with the predictions of Grodstein,[1] the experimental results are consistently higher. The Grodstein values were obtained with a slightly inaccurate pair cross section, Votruba triplet cross section, and a Klein-Nishina Compton cross section. Each cross section choice will receive comment.

An increase of the pair cross section values, as de-

[32] Montalbetti, Katz, and Goldemberg, Phys. Rev. **91**, 659 (1953).
[33] J. Halpern and A. K. Mann, Phys. Rev. **83**, 370 (1951).

scribed in Sec. VA1, can be justified for three separate reasons. First, the experiment performed with equal numbers of electrons per square centimeter in a carbon and aluminum attenuator required about a 2% increase in the pair cross-section values at 60 Mev. Second, the triplet cross section is not a large enough fraction of the total cross section in carbon and aluminum attenuators at 60 Mev to be able to explain the discrepancy between the Grodstein value and the experiment. Therefore the pair cross section is suspect. Third, the high-energy experimental results (60–300 Mev) on total attenuation cross sections summarized by Malamud[16] are almost all larger by 1 to 3% than the theoretical predictions for high atomic number attenuators where the pair cross sections predominate.

Unfortunately, no theoretical reason is available to explain the 2.25% increase in pair cross section that was used in the present interpretations. Therefore, it was assumed that the increase was independent of energy and it was applied to the pair coefficients for carbon, water, and aluminum. No increase in pair cross section was assumed in the case of hydrogen.

If the increase in the pair cross section is accepted and the validity of the uncorrected Klein-Nishina Compton cross section is assumed, then the remainder cross section may be evaluated as a triplet cross section. This type of comparison has been made in Table VI at 60 Mev for hydrogen, carbon, water, and aluminum. Also listed are each of the calculated triplet cross sections illustrated for carbon in Fig. 10. The conclusion to be drawn from this comparison is that the Votruba[13] triplet cross section is too small and outside the limits of the present interpretations. On the other hand the Borsellino[19] triplet predictions permit a good comparison with the experiment.

The assumption that the Compton cross section is given by the Klein-Nishina formula might be incorrect because of the radiative corrections calculated by Brown and Feynman.[21] For carbon, water, and aluminum at 60 Mev the Compton cross sections are a relatively small part of the total cross sections. However, the total cross section in hydrogen is predominantly affected by the Compton cross section. In this case [Fig. 7(a)], the experimental results are, within the experimental uncertainties, the same as the predicted cross sections obtained with the Klein-Nishina Compton, the Bethe-Heitler pair, and the Borsellino triplet cross sections. Therefore, this result suggests that corrections to the integrated Compton cross section are small.

TABLE VI. Triplet calculation at 60 Mev in millibarns.

	Hydrogen	Carbon	Water	Aluminum
Exp. total[a]	21.71±0.21	287.28±0.60	502.39±1.7	1064.5±2.4
Compton	12.54	75.2	125.4	163.0
Corrected pair	5.1	182.8	332.1	840.9
Remainder "triplet"	4.07±0.21	29.20±0.60	45. ±1.7	60.6±2.4
Votruba triplet	3.3	20	29	42
Borsellino triplet	4.5	27	45	58
(1/Z) Xpair	5.1	30.5	41.5	64.7
Wheeler and Lamb	5.2	31	52	68
W-L with exchange	3.5	21	35	45

[a] Only statistical errors have been indicated in this table.

B. Total Cross Sections in the Energy Range of 13 to 18 Mev

Though the experimental results are about 1% higher than the predictions in this region, the large uncertainties arising from the response function correction factors and energy assignments make the agreement within the experimental uncertainties. The biggest disagreement is with the recent nuclear detector data of Bergsteinsson *et al.*[34] who found experimental values at 14 to 20 Mev that were lower than the present experiment; this difference is not presently understood.

C. Pulse-Height Predictions

The comparison in Fig. 8 of the predicted and experimental pulse-height distributions obtained without an attenuator was a consistency check of the response function matrix and the assumed spectrum. The spectrum was taken to be that predicted by Davies, Bethe, Maximon[2] with a target thickness correction suggested by Hisdal.[35] In addition, the distributions obtained with a carbon attenuator, as shown in Fig. 9, permitted a detailed test of the assumed attenuation coefficients in the giant resonance region. Small trial deviations from the experimental nuclear absorption coefficients as plotted on Fig. 7, led to rather large departures from the experimental curve of Fig. 9. The comparisons in both Figs. 8 and 9 are good except for the details at the high-energy end of the spectrum where the data are dependent on the accuracy of the response function information. For example, both experiments plotted in Figs. 8 and 9 were made with a nominal 35-Mev synchrotron energy. In obtaining a best fit to these distributions it was necessary to use 35.3 Mev as the peak energy for the no-attenuator experiment, while 34.3 Mev gave the best fit for the carbon-attenuator experiment shown in Fig. 9. These different energy values probably indicate the lack of an accurate response function shape in the 35-Mev region and the problem of fitting a distribution which approaches the base line asymptotically. In order to demonstrate the independence of the results in the giant resonance energy region on the peak energy values, the 35.3-Mev spectrum has been plotted on Fig. 9 for comparison.

D. Nuclear Cross Sections

The least accurate results from this experiment are the total nuclear attenuation cross sections, since they result from the subtraction of an uncertain electronic contribution from the total attenuation cross section. In addition, the response function of the spectrometer,

[34] Bergsteinsson, Robinson, Siddiq, Horsley, and Haslam, Can. J. Phys. **36**, 140 (1958).
[35] E. Hisdal, Phys. Rev. **105**, 1821 (1957).

which has a full width at half maximum of 15% at 22 Mev, cannot be expected to resolve fine structure or rapid variations in the nuclear cross section. However, it is believed significant comments can be made about the differential and integrated cross sections.

The differential nuclear cross sections are given by the curves of Fig. 11 for carbon, oxygen, and aluminum and are labeled "experiment." These cross sections are uncertain by about $\pm 15\%$ in the giant resonance and high-energy tail regions largely because of the uncertainties in the removal of the electronic contributions to the total cross section. However, the experimental nuclear cross sections should be systematically in error as a function of the atomic number of the attenuator. For example, the electronic contribution was removed by subtracting the sum of the Compton, triplet, and an increased pair cross section. The factor of increase for the pair cross section was 1.0225. If this factor at 22 Mev should have been smaller then all of the nuclear cross sections would be larger. Therefore, the fact that the carbon cross sections (synthesis and this experiment) at the peak of the giant resonance agree, and that carbon has been examined in great detail by previous experiments, suggests that the discrepancy for oxygen is real. In addition, the increase in the oxygen total nuclear cross section above the synthesized value is consistent with the oxygen scattering results of Garwin and Penfold.[36]

The differential nuclear cross sections measured by Ziegler,[37] and Kockum and Starfelt[38] for aluminum by a total attenuation technique similar to that of the present experiment are somewhat smaller than cross sections obtained in this experiment. The results of Mihailović *et al.*[39] are considerably larger.

The integrated cross sections obtained from the areas under the curves of Fig. 11 have been compared in Table VII with the cross sections calculated by use of the Gell-Mann, Goldberger, and Thirring[40] sum rule:

$$\int_0^{\mu} \sigma dk = (0.06NZ/A)[1+(0.1A^2/NZ)] \text{ Mev barns}, \quad (3)$$

where μ is the energy of the photomeson threshold. The same integrated cross section for carbon, oxygen, and aluminum was obtained using slightly different approximations by the earlier work of Levinger and Bethe[41] when the fraction of attractive exchange force, x, in their model was assumed to be 0.5. The sensitivity of the experimental value of the integrated nuclear cross section is demonstrated in the table by the reduction of the integrated cross section for carbon by 13% when the pair correction factor is increased from 1.0225 to 1.03. Partly because of this sensitivity, the assigned uncertainty to the experimental integrated cross sections is $\pm 15\%$. Therefore, the oxygen and aluminum integrated cross sections may be considered to agree with the theoretical sum rules while the carbon value is somewhat higher than expected.

TABLE VII. Integrated cross sections in Mev barns, sum rule comparisons.

	$K=1.0225$			$K=1.03$
	Carbon	Oxygen	Aluminum	Carbon
Nuclear	0.267	0.191	0.373	0.219
Quenched quasi-deuteron	0.110	0.141	0.233	0.110
Total	0.377	0.332	0.606	0.329
G-G-T sum rule	0.252	0.341	0.567	0.252
Ratio: Total exp./Sum rule	1.50	0.974	1.069	1.31

VII. CONCLUSIONS

The principle on which the present experiment was based was the simultaneous recording of all x-ray energies in a spectrum transmitted by very long attenuators. The long attenuators that could be used because of the high sensitivity of the sodium iodide spectrometer permitted the accurate determination of attenuation coefficients, particularly when the coefficients varied little with photon energy.

Two main conclusions may be drawn from these determinations. The first is that the total attenuation coefficients at 60 Mev for carbon, water, and aluminum are higher than would be predicted. The source of the discrepancy is not fully understood, although the pair production cross section is suspect. A 2.25% increase in the pair production cross sections at 60 Mev made the results agree with theory.

The second conclusion concerns the nuclear cross sections above about 25 Mev. At these energies the total cross section varies slowly and can be determined accurately. The nuclear cross section results from a subtraction of an uncertain electronic contribution from the total cross section. However, if the procedures used in the paper for subtraction of the electronic contribution are valid, then it must also be concluded that the high-energy tails of the nuclear cross sections are determined to better than $\pm 15\%$ and that the cross sections above 25 Mev are considerably larger than would be predicted from a synthesis of previous photoneutron and photoproton experiments. When the inadequacies of the theoretical information on the corrections to the Compton, pair, and triplet cross sections are resolved, more reliable data on the total nuclear absorption shapes can be obtained from the present results.

[36] E. L. Garwin and A. S. Penfold, Bull. Am. Phys. Soc. Ser. II, 4, 288 (1959).
[37] B. Ziegler, Physik **152**, S. 566 (1958).
[38] J. Kockum and N. Starfelt, Nuclear Instr. **5**, 37 (1959).
[39] Mihailović, Pregl, Kernel, and Kregar, Phys. Rev. **114**, 1621 (1959).
[40] Gell-Mann, Goldberger, and Thirring, Phys. Rev. **95**, 1612 (1954).
[41] J. S. Levinger and H. A. Bethe, Phys. Rev. **78**, 115 (1950).